BAAA, Vol. 63, 2022
R.D. Rohrmann, M.N. Gómez, C.E. Boeris & M.A. Sgró, eds.

Asociación Argentina de Astronomía
Boletín de artículos científicos

Search for rapid radio variability in a sample of gamma-ray emitting blazars with the radio telescopes of IAR

C.A. Galante[1,2], G.E. Romero[1,2] & G.A. Gancio[2]

[1] *Facultad de Ciencias Astronómicas y Geofísicas, UNLP, Argentina*
[2] *Instituto Argentino de Radioastronomía, CONICET–CICPBA–UNLP, Argentina*

Contact / camigalante04@gmail.com

Resumen / Los blazares –núcleos galácticos activos con uno de los jets apuntando al observador– muestran variaciones en su densidad de flujo a lo largo de todo el espectro electromagnético sobre escalas de tiempo que van de minutos a años. La emisión de rayos gamma en estos objetos indica la presencia de poblaciones de partículas relativistas. Dichas partículas deberían además emitir en radio frecuencias por mecanismo sincrotrón. La investigación de la microvariabilidad en longitudes de onda de radio puede proveer información sobre los procesos no térmicos que ocurren dentro de los jets. Presentamos aquí resultados de observaciones de variabilidad a 1.4 GHz de una muestra de blazares, seleccionados debido a su fuerte emisión en rayos gamma. La campaña observacional se llevó a cabo durante febrero de 2021 utilizando el telescopio renovado Esteban Bajaja ubicado en el Instituto Argentino de Radioastronomía.

Abstract / Blazars – active galactic nuclei in which one of the jets is pointing toward the observer – show flux density variations throughout the entire electromagnetic spectrum on time scales ranging from minutes to years. The occurrence of gamma-ray emission in these objects indicates the presence of populations of relativistic particles. Such particles should also emit in radio frequencies by synchrotron mechanism. The investigation of microvariability at radio-wavelengths can provide information about the non-thermal processes that occur inside the relativistic jets. We present results of 1.4-GHz variability observations of a sample of blazars, selected because of their strong gamma-ray emission. The observational campaign was carried out in February, 2021, using the upgraded Esteban Bajaja radio telescope of the Instituto Argentino de Radioastronomía.

Keywords / galaxies: active — Galaxy: general — radiation mechanisms: non-thermal — radio continuum: galaxies

1. Introduction

Active Galactic Nuclei (AGN) are found at the centers of numerous galaxies. The standard model describes them as supermassive black holes, with masses greater than 10^7 $M_\odot$, surrounded by an accretion disc and a dusty torus (Rees, 1984). In many cases, perpendicular to the disc, two jets of relativistic plasma are ejected. When these jets are pointing close to the line of sight to the observer, the AGN is classified as a blazar. The particles in the jets are injected into the interstellar medium at relativistic speeds. In consecuence, the radiation of the jet pointing to the observer will be amplified by Doppler effect. The jets are far from thermal equilibrium, making the non-thermal radiation mechanisms the dominating ones. In particular, at radio frequencies the emission is originated via synchrotron process.

Two of the main characteristics observed in blazars at radio wavelengths are the variability of their flux densities and a high degree of polarization, which is also variable. In the past, variations in the flux density have been observed by many authors on time scales ranging from minutes to years. The causes of the rapid variability –the one we are studying in this work– could be extrinsic, such as interstellar scintillation (Rickett, 1986) or gravitational microlenses (Nottale, 1986; Gopal-Krishna & Subramanian, 1991), or intrinsic, as the presence of shocks inside the jets (Romero et al., 1995b; Webb, 2016).

2. Sources and instrument

The sources selected for our observations are two southern BL-Lac blazars: PKS 0521-365 ($z = 0.056$) and PKS 1921-293 ($z = 0.353$). Both objects have been observed in radio, optical, UV, and at high energies, in X-rays with *Chandra* and gamma rays first with EGRET and then with *Fermi-LAT*. Furthermore, they have shown variability in their emission and have been observed with IAR telescopes in the past (Romero et al., 1995a), showing a mean flux density of 17.9 Jy and 11.5 Jy respectively. The flux densities of the calibration sources PKS 0320-37 ($z = 0.0058$) and PKS 1610-60 ($z = 0.0181$) at $\nu = 1.4$ GHz, taken from Testori et al. (2001), are $F_\nu = 82.5$ Jy and $F_\nu = 60$ Jy, respectively. These sources were chosen because they are well studied and show a non-variable flux density at radio frequencies.

The instrument used in this work was the Esteban Bajaja radio telescope, located at the IAR. It has a diameter of 30 m and an angular resolution of 30 arcmin when operating at 1.4 GHz. It underwent an upgrade

Poster contribution

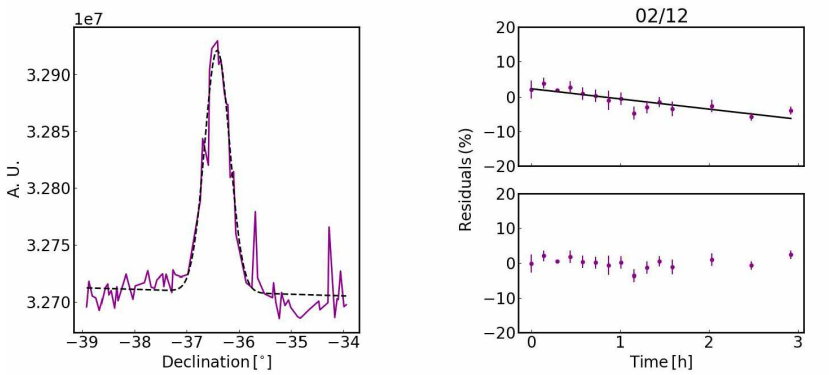

Figure 1: *Left panel*: Example of a declination scan for PKS 0521-365. *Right panel*: Intraday lightcurve and correction for PKS 0320-37.

process in 2018-2019, including the implementation of digital receivers that allow working with greater instantaneous bandwidth (56 MHz) and higher sensitivity. The total tracking time for a source is 220 minutes, and the range of observable declinations are between $-90°$ and $-10°$. The central frequency is 1300 MHz, with a bandwith of 300 MHz. The reciever temperature is 90 K and the gain is 12 Jy K^{-1}. The front-end allows to obtain both circular polarization products, while the back-end consists of two SDR boards that can be used as consecutive bands for a given polarization or to obtain both polarization modes. Currently it is the second configuration that is used.

3. Observational campaign and data reduction

We made the observations daily between February 9 and 18, 2021, including both blazars and the two calibrating sources each night. To automate the observations, bash scripts were built for each day. The measurements were obtained by means of declination scans with an amplitude of 2.5° towards each side and a duration of 2 minutes. Previously it was verified that the pointing in right ascension is accurate.

Each scan was fitted by a function composed of a Gaussian plus a linear function that models the baseline. The signal from the source corresponds to the maximum of the Gaussian. In order to improve the signal-to-noise ratio, each measurement was obtained from the average of 6 scans. The error that affects these measurements has two components: one proportional to intensity (errors in antenna positioning, changes in gain, etc.) and another independent of intensity (detector noise, external interference). Flux calibration was performed using the values indicated in Section 2 for the calibration sources.

4. Results and variability analysis

A similar negative slope was found for all days in the intra-day lightcurves of PKS 1610-60, while for PKS 0320-37 the effect was only noticeable in two days and it was corrected (see Figure 1-right). For this reason only PKS 0320-37 was used for flux calibration. The observed slopes are an indication of systematic errors in the instrument, which must be studied in depth to determine their origin. Most likely they are mechanical tracking problems depending on the declination. Moderate variability on timescales of days was found for PKS 0521-365 (Figure 2-left) while systematic errors prevented any firm conclusion on PKS 1921-293 (Figure 2-center). A mean flux density of 4.58 Jy was obtained for PKS 1921-293 and 12.2 Jy for PKS 0521-365, in both cases with errors less than 10%. The values for each day are shown in Table 1.

PKS 0521-365				PKS 1921-293			
Day	$< F_\nu >$	ϵ_S	n	Day	$< F_\nu >$	ϵ_S	n
09	11.61	0.41	13	12	4.92	0.33	12
11	10.39	0.44	11	13	5.10	0.38	12
12	13.05	0.49	14	14	4.64	0.41	12
13	12.75	0.54	11	16	4.54	0.31	14
15	12.32	0.48	15	17	4.20	0.42	14
16	12.51	0.53	14	18	4.10	0.25	9
17	12.77	0.66	14				

Table 1: Main parameters of the observations. For each source, the first column corresponds to the observation day, the second and the tird are the flux density in Jy and its error, and the last one is the number of observations for each day.

We calculated multiple variability parameters for PKS 0521-365. First, the fluctuation indices (Figure 3-left), given by $\mu = 100\epsilon_S / < S >$, give an estimate of the dispersion of the observations with respect to their weighted mean value. Second, the variability amplitudes (Figure 3-center) are defined as $Y = 3\sqrt{\mu^2 - \mu_{cal}^2}$, where μ_{cal} is the fluctuation index for the calibration source, and the fractional variability (Figure 3-right) is given by $FV = (S_{max} - S_{min})/(S_{max} + S_{min})$, where S_{max} and S_{min} are the maximum and minimum values of S respectively. Finally, we calculated the Discrete Auto-correlation Functions (ACF), based in the method

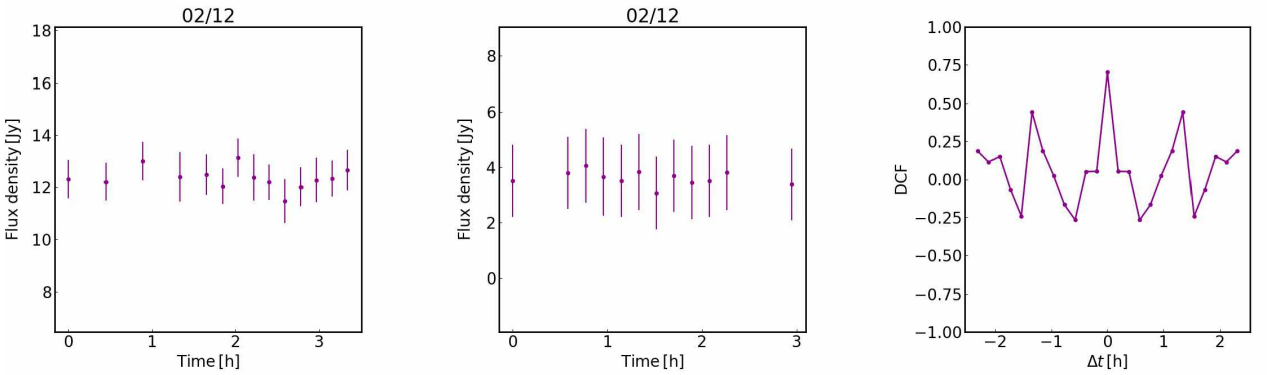

Figure 2: *Left panel*: Intraday lightcurve for PKS 0521-365. *Center panel*: Intraday lightcurve for PKS 1921-293. *Right panel*: Discrete autocorrelation function for PKS 0521-365.

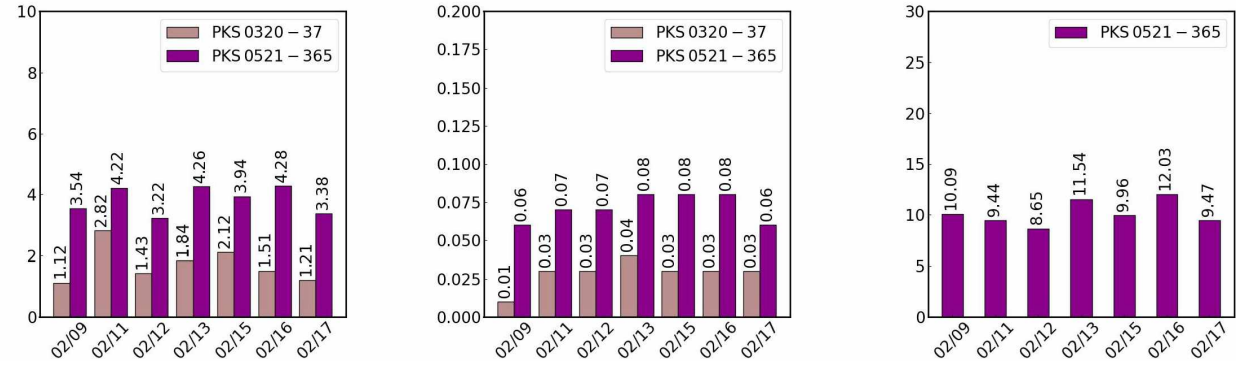

Figure 3: *Left panel*: Fluctuation indices comparison. *Center panel*: Fractional variability comparison. *Right panel*: Variability amplitudes for PKS 0521-365.

developed by Edelson & Krolik (1988). The variability time scales are shown as minima in the ACF, while the existence of maxima indicates possible periodicities or quasi-periodicities. The ACF obtained for PKS 0521-365 show minima at $\Delta t \sim 36$ minutes, produced by the temporal resolution of the observations, and in some cases between 1-2 hours, but we were unable to define a unique time scale. On the other hand, for this source, we found an interday variability time scale of 6.5 days, given by $\tau_v = S_{\max}\,(\Delta S/\Delta t)^{-1}$. Finally, we performed an F-test to determine the intra-day and interday variability, and we could reject the non-variability hypothesis only for days 02/15 and 02/16. This result could be a consecuence of the slope found in the lightcurves of the calibration sources, that may be masking the intrinsic variability if present on the remaining days with smaller amplitudes.

5. Conclusions and future work

We performed the first continuum observations with IAR radiotelescopes in 20 years. Our work has shown the necessity of an in-depth characterization of the systematic errors found in the radiotelescope to remove them efficiently from future observations. In the future, we intend to extend the duration of the campaigns, expand the sample of objects and obtain polarization data. In addition, we plan to extend our investigation making use of facilities such as the ESA's Deep Space Antenna 3 and the CLTC-CONAE-NEUQUEN station.

References

Edelson R.A., Krolik J.H., 1988, ApJ, 333, 646
Gopal-Krishna, Subramanian K., 1991, Nature, 349, 766
Nottale L., 1986, A&A, 157, 383
Rees M.J., 1984, ARA&A, 22, 471
Rickett B.J., 1986, ApJ, 307, 564
Romero G.E., Benaglia P., Combi J.A., 1995a, A&A, 301, 33
Romero G.E., Combi J.A., Vucetich H., 1995b, Ap&SS, 225, 183
Testori J.C., et al., 2001, A&A, 368, 1123
Webb J., 2016, Galaxies, 4, 15